Hydrology Research

Hydrology Research Vol 53 No 1, 241 doi: 10.2166/nh.2021.192

A new method for dividing flood period in the variable-parameter Muskingum models

Reyhaneh Akbari* and Masoud-Reza Hessami-Kermani

Department of Civil Engineering, Shahid Bahonar University of Kerman, Kerman, Iran
*Corresponding author. E-mail: r.akbari@ymail.com

ABSTRACT

The Muskingum routing model is favored by water engineers owing to its simplicity and accuracy. A large amount of research is done to improve the accuracy of the model. One way to do so is to consider variable hydrological parameters during the flood routing period. In this study, the random selection (RS) method was proposed to divide the flood period of the nonlinear Muskingum model into three sub-periods. The proposed method was based on RS of members in each sub-region. It was applied to rout three flood hydrographs, and the objective function was the sum of squared errors. Comparing the results from the three variable-parameter nonlinear Muskingum model with those from the variable-parameter nonlinear Muskingum models in previous studies, the proposed model optimized the objective function in these hydrographs up to 61%. The uncertainty analysis of Muskingum parameters for Wilson's hydrograph was performed by the fuzzy alpha cut method, and it was found that the uncertainty of the parameter x is greater than the uncertainty of the parameters k and m.

Key words: Muskingum model, parameter estimation, particle swarm optimization-genetic algorithm, random selection, river routing, uncertainty

HIGHLIGHTS

- A new random selection method was used to increase the accuracy of the variable-parameter Muskingum model.
- The PSO–GA algorithm was used to estimate the Muskingum parameters.
- The proposed model was applied to three examples, and the results showed that this model has estimated the outflows more accurately in all three examples than the previous methods.
- The fuzzy alpha cut method was used to quantify the uncertainty of Muskingum parameters.

INTRODUCTION

Flood routing is a procedure to determine the time and magnitude of a flow. The flow hydrograph at a point on a watercourse is determined using known or assumed hydrographs at one or more points upstream. Flood routing is an effective step toward flood prediction and control and can reduce its harmful consequences. Flood routing is classically done in two main ways: hydraulic flood routing and hydrologic flood routing (Barati 2013). Among hydrologic routing methods, the Muskingum method is very popular with researchers and water engineers on account of its ease of use and simplicity. In addition, the Muskingum model makes accurate predictions with fewer data types than common hydraulic methods (Barati 2013). This method can be used to determine flood hydrographs in places with similar morphological aspects (Bazargan & Norouzi 2018), whereas it cannot be employed in cases where significant backwater effects are observed (Chow *et al.* 1988). Some researchers have considered constant parameters for the Muskingum model, while some have used the variable ones. Clearly, the Muskingum model is called 'constant-parameter' as long as the parameters are considered constant during the routing period, while, if these parameters are considered variable during the routing period, the Muskingum model is called a 'variable-parameter Muskingum model'.

The determination of the parameters of the Muskingum model has been a topic of research for many years. Gill (1978) implemented the segmented curve method for nonlinear flood routing, in which the least squared error was taken advantage of so as to estimate the parameters. Among optimization methods, the evolutionary algorithms have been used to ascertain the parameters of the Muskingum model owing to their high accuracy, as well as their capability of solving multi-variable problems. In this regard, Mohan (1997) employed a genetic algorithm (GA), and Kim *et al.* (2001) used a harmony search (HS) method to estimate the parameters of the Muskingum model. Chu & Chang (2009) determined the parameters of the model using the particle swarm optimization (PSO) method, whereas Luo & Xie (2010) took advantage of the

immune clonal selection algorithm to determine the parameters. The hybrid model, combining HS and PSF methods (parameter-setting-free HS), was introduced by Geem (2011) to deal with complex systems. It is noteworthy to emphasize that, this way, 5,000 functions are optimized in only 1 s. Karahan *et al.* (2012) proposed a hybrid model of HS and Broyden–Fletcher–Goldfarb–Shanno algorithm methods and compared the results from the proposed model with those from eleven other methods. Hamedi *et al.* (2016) developed a nonlinear Muskingum model by introducing a parametric initial storage condition and applied the weed optimization algorithm to route the flood. Niazkar & Afzali (2017b) proposed a hybrid model of the modified honey bee mating and generalized reduced gradient (GRG) algorithms to develop a nine constant-parameter Muskingum model. Qiang *et al.* (2020) and Yuan *et al.* (2021) utilized the whale optimization algorithm with elite opposition-based learning and Polak–Ribière–Polyak methods, respectively, to route the flood in the Haihe River. Norouzi & Bazargan (2020, 2021) applied the PSO method to optimize the Muskingum parameters of the model. Okkan & Kirdemir (2020) routed four flood hydrographs using PSO to optimize the Levenberg–Marquardt model. Khalifeh *et al.* (2020b) managed to route the flood in the Kardeh River by the grasshopper optimization algorithm and compared the results from the model with the ones from GA and HS algorithms. Not only have the researchers employed a variety of algorithms, but they have also suggested different structures for the Muskingum model in order to improve the precision of the model in estimating the Muskingum parameters. Khalifeh *et al.* (2020a) implemented a Muskingum model with seven variables for flood routing in Karun River, in which the parameters were determined by the symbiotic organisms search algorithm. Bozorg-Haddad *et al.* (2020) utilized a 15-parameter Muskingum equation and employed the Excel Solver in order to optimize the outflow coefficient. They assumed the coefficient as a factor of the inflow rate. The results showed that although this adds to the complexity of the model, it ends in much more precise results.

The variable-parameter Muskingum model has been introduced as an approach to improve the results. The nonlinear variable-parameter Muskingum model was first used in the case of three flood hydrographs by Easa (2013), in which the exponential parameter was set to be variable. Niazkar & Afzali (2017a) and Afzali (2016) split the flood period into two and three sub-regions, where a unique parameter was studied for each. Zhang *et al.* (2017) used an improved real-coded adaptive GA (RAGA) with an elite strategy for precise parameter estimation of the nonlinear Muskingum model. They divided the flood period into five sub-regions. Kang & Zhou (2018) and Akbari *et al.* (2020) specified all Muskingum parameters, associated with the flood period, for three sub-regions and showed that the sum squared deviation (SSQ) significantly decreased using the introduced model. Bazargan & Norouzi (2018) determined k, x, and Δt parameters for the first hydrograph and then calculated the outflows for the second hydrograph based on the parameters calculated for the first one. They divided the flood period into three sub-regions and considered Muskingum parameters variable.

The present study aims to increase the accuracy of the Muskingum model. In this regard, a new method for dividing the flood period into a number of sub-regions in the variable-parameter Muskingum model is proposed. Different methods have so far been used to divide the flood hydrograph period into sub-regions based on the time, or the inflow hydrograph, and the peak flows. In this research, the random selection (RS) method has been utilized to divide the flood period. The efficiency of the RS method has been evaluated by routing three flood hydrographs, including Wilson's hydrograph, O'Donnell hydrograph, and a flood hydrograph in a river with the same morphological aspect as the Karun River, located in Iran. In order to assess the predictive ability of the present model, evaluative measures were used for these hydrographs. The performance of the present model was compared with that of the models from the literature. The values of objective function have been decreased by 5% in the first case study, compared to the nonlinear Muskingum model with eight constant parameters. The values decreased by 61% in the second case study, compared to the nonlinear Muskingum model with four-variable parameters. In the third case study, the objective was optimized by 96%, compared to the Muskingum model with three constant parameters. The Muskingum equations related to all models have been presented in Tables 3, 5 and 7. This does indicate an improvement in the accuracy and efficiency of the proposed model and proves that the RS method can be an attractive alternative. The uncertainty of the Muskingum parameters obtained using the RS method was examined in Wilson's hydrograph by the fuzzy alpha cut (FAC) method. It was found that the uncertainty of parameter x is greater than that of parameters k and m.

METHODS

The Muskingum model is formed on account of the relationship between the storage, and weighted inflow and outflow. Based on the nonlinear relationship between these two factors, different forms of the nonlinear Muskingum model have been created, which are presented in Niazkar & Afzali (2016).

In this paper, a three-parameter nonlinear Muskingum model, whose Muskingum parameters vary during the routing period, is employed as follows:

$$S_t = k_t(x_t I_t + (1 - x_t)O_t)^{m_t} \tag{1}$$

The continuity Equation is written in the following fashion:

$$\frac{dS_t}{dt} \approx \frac{\Delta S_t}{\Delta t} = I_t - O_t \tag{2}$$

Considering Equations (1) and (2), the outflow is determined by the following equation:

$$O_t = \left(\frac{1}{1 - x_t}\right)\left(\frac{S_t}{k_t}\right)^{\frac{1}{m_t}} - \left(\frac{x_t}{1 - x_t}\right)I_t \quad t = 2, 3, \ldots, T \tag{3}$$

The rate of storage changes with time is calculated by substituting Equation (3) into Equation (2):

$$\frac{\Delta S_t}{\Delta t} = -\left(\frac{1}{1 - x}\right)\left(\frac{S_t}{k}\right)^{\frac{1}{m}} + \left(\frac{1}{1 - x}\right)I_t \quad t = 2, 3, \ldots, T \tag{4}$$

The storage in the next step is calculated by the following equation:

$$S_t = S_{t-1} + \frac{dS_t}{dt}\Delta t \quad t = 2, 3, \ldots., T \tag{5}$$

The outflow can be determined using Equation (3) in the next step (Kang & Zhou 2018).

Moreover, in this research, the objective is set to be minimizing the sum of the squared errors:

$$\text{Minimize SSQ} = \sum_t [O_t - \hat{O}_t(k,\ x,\ m)]^2 \tag{6}$$

In addition, the other performance indicators of SAD, VarexQ, EQp, ETp, and MARE were taken advantage of as follows in order to compare the results from the proposed method to the ones from the methods in other works of research:

$$\text{SAD} = \sum_{t=1}^{T} |O_t - \hat{O}_t| \tag{7}$$

$$\text{ET}_\text{p} = |T_\text{p} - \hat{T}_\text{p}| \tag{8}$$

$$\text{EQ}_\text{p} = \frac{|O_\text{p} - \hat{O}_\text{p}|}{O_\text{p}} \tag{9}$$

$$\text{MARE} = \frac{1}{N}\sum_{t=1}^{T} \frac{|O_t - \hat{O}_t|}{O_t} \tag{10}$$

$$\text{VarexQ} = \left[1 - \frac{\sum_{t=1}^{T}(O_t - \hat{O}_t)^2}{\sum_{t=1}^{T}(O_t - \bar{O}_t)^2}\right] \times 100 \tag{11}$$

where O_p represents the observed peak outflow, and $\hat{O}_\text{p}$ stands for the calculated peak outflow. T_p and $\hat{T}_\text{p}$ constitute the time of the observed peak outflow and the time of calculated peak outflow, respectively. Moreover, $\bar{O}_t$ represents the mean of the observed outflow. The lower the value of EQ_p, the more accurate the model. Plus, the smaller the value of

ET_p, the more accurate the prediction of peak discharge. The proximity of the shape and the size of the hydrograph are measured using Equation (11) (Moghaddam *et al.* 2016).

The choice of the objective function has a direct effect on flood routing results. Many researchers have chosen SSQ as the objective function (Akbari *et al.* 2020), whereas some others have gone for the SAD (Norouzi & Bazargan 2021). However, both have been chosen as the objective function in some cases (e.g., Orouji *et al.* 2013), making it a two-objective optimization problem.

Optimization algorithm

Genetic algorithm

The optimization in GA is performed through crossover and mutation, presented in the following equations:

$$\begin{cases} X_{t+1}^{i} = c_i.X_t^i + (1-c_i)X_t^{i+1} \\ X_{t+1}^{i} = (1-c_i)X_t^i + c_i.X_t^{i+1} \end{cases} \tag{12}$$

$$X_{t+1}^{i} = X_t^i + c_i' \tag{13}$$

X_t^i and X_t^{i+1} form a pair of population members before the crossover, whereas X_{t+1}^i and X_{t+1}^{i+1} are a pair after the crossover. c_i is a random number between 0 and 1 (Wu *et al.* 2015).

The steps of exchanging genetic information are repeated until the algorithm terminates.

PSO algorithm

The PSO is a swarm intelligence algorithm, which is based on the social behavior of birds and fish to find food. First, particles with different velocities and positions are randomly generated in the search space. Each particle, then, updates its position and velocity based on the particle's own experience and the best experience of the population. On condition that $|v_i^t| \le V_{\max}$, the velocity and position of the particles are updated by Equations (14) and (16) in each iteration (Xu *et al.* 2019):

$$v_{t+1}^{i} = \chi[v_t^i + c_1 \cdot \mathrm{Rand}(\cdot) \cdot (\mathrm{pbest}_t^i - x_t^i) + c_2 \cdot \mathrm{Rand}(\cdot) \cdot (\mathrm{gbest} - x_t^i)] \tag{14}$$

$$\chi = \frac{2}{\left|2 - \varphi - \sqrt{\varphi^2 - 4\varphi}\right|} \quad \varphi = c_1 + c_2, \quad \varphi > 4 \tag{15}$$

$$x_{t+1}^{i} = x_t^i + v_{t+1}^i \tag{16}$$

where c_1 and c_2 represent the social parameters 1 and 2, and are both considered 2.05 in this research. In addition, x is the constriction coefficient, which is a function of c_1 and c_2. Rand(·) acts for a random positive number that is calculated by a uniform distribution between 0 and 1. pbest_t^i is the best position particle 'i' has ever been in. x_t^i and v_t^i are the position and velocity of the ith particle in the tth iteration in the search space. After all, gbest_t^i is the best position of the whole population.

PSO–GA algorithm

Gaining the advantages of both algorithms, while avoiding the disadvantages of each, the theory of a new hybrid algorithm was developed. The PSO and GA algorithms have their own advantages and disadvantages, which are used in combination with each other, can lead to increasing the advantages and lowering the disadvantages. In the previous section, the steps of PSO and GA algorithms were separately described. The PSO–GA algorithm optimizes Muskingum parameters with a high convergence rate and a significant accuracy. In this method, Muskingum parameters or so-called 'the agents' are randomly generated in the search space at first, and then the steps of the PSO algorithm are executed, through which the velocity and position of the particles are updated. In the following step, the next generation is created by comparing the population's best experience with the particle's best experience. Now, the crossover and mutation are applied to the new population and the members of the new population are sorted according to the objective function. The succeeding generation is produced by comparing the population and particle's best experience. Provided that the termination condition is satisfied, the results are reported as outcomes of the algorithm. Otherwise, the steps of the algorithm continue until the termination condition of the algorithm is reached (Garg 2016). The steps of the hybrid PSO–GA algorithm are illustrated in Figure 1.

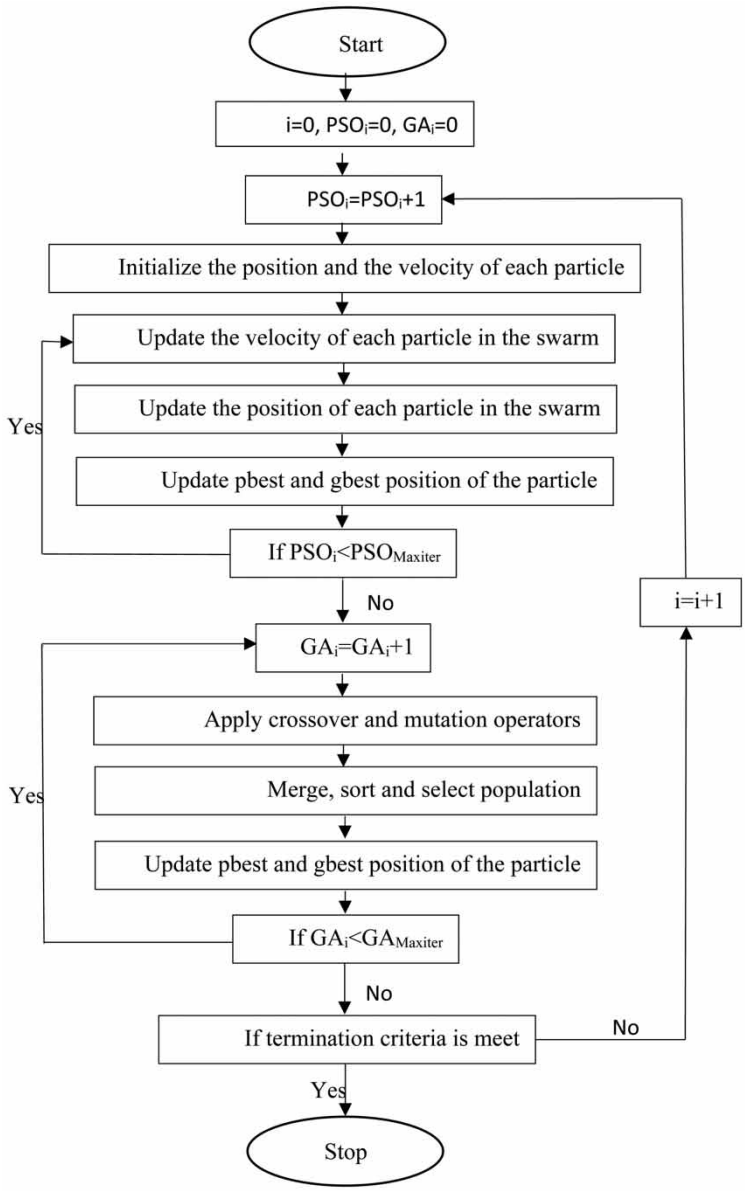

Figure 1 | Hybrid PSO–GA algorithm (Akbari *et al.* 2020).

RS method

Suppose I_i points are to be divided into three categories, the points that are placed in categories 1, 2, and 3 are given the values (k_1, x_1, m_1), (k_2, x_2, m_2), and (k_3, x_3, m_3), respectively. First, the values (k_1, x_1, m_1), (k_2, x_2, m_2), and (k_3, x_3, m_3) are randomly generated in the search space. In the next step, points I_i, $i = 1, \ldots, J$ are randomly assigned to each of the categories 1, 2, and 3. At this stage, the number of members in each category is not a fixed number, but the sum of the members of the three categories needs to equal J. Afterwards, the flow routing operation is performed. Now as shown in Figure 2, for each I_i, there is a specific value (k, x, m) depending on which of the categories 1, 2, and 3 is located in, and then the outflows are calculated using it, and the SSQ is obtained. Generating values of (k_1, x_1, m_1), (k_2, x_2, m_2), and (k_3, x_3, m_3) are performed using the optimization algorithm and assigning I_i points to categories 1, 2, and 3. This way, the SSQ is calculated. Likewise, the whole process continues until the optimization algorithm termination condition is satisfied.

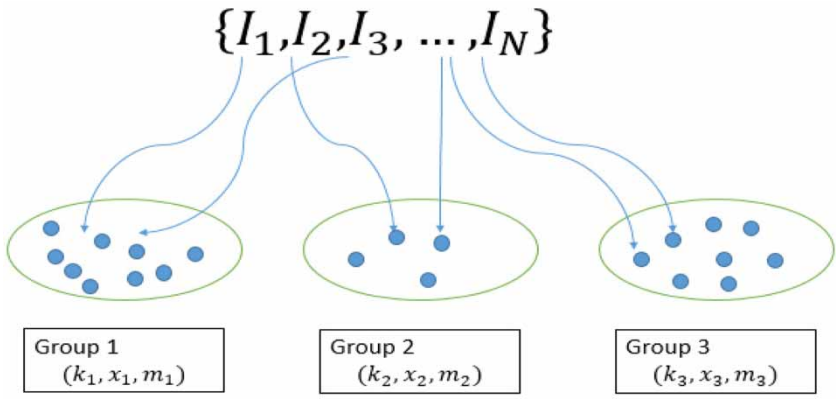

Figure 2 | Division of the flood period into three sub-regions and the specification of hydrological parameters for each category.

Uncertainty

Uncertainty analysis depends on many elements, such as knowing the origins of uncertainty and the complexity of the model. In order to determine the uncertainty of the models, the possibility theory is used in the case of exact and quantitative measurements, while the probability theory is taken advantage of for qualitative and rough measurements. Due to the simplification of equations and/or the use of random variables, the quantitative estimation of parameters is always accompanied by uncertainty. Quantifying the uncertainty is one of the ways to determine the uncertainty. It uses the triangular fuzzy membership numbers. In this method, the membership value of the maximum and minimum is assigned 0, while 1 is assigned to the median so as to lower the impact of the scattered data.

$$\mu(s) = \begin{cases} \dfrac{s - s_1}{s_2 - s_1} & s_1 < s < s_2 \\ \dfrac{s_3 - s}{s_3 - s_2} & s_2 < s < s_3 \\ 0 & \text{Other values} \end{cases} \tag{17}$$

$$U = \frac{(S_3 - S_1)*0.9}{S_2} \tag{18}$$

where s is the intended variable; $\mu(s)$ represents the membership degree of the variable s. s_1 is the minimum value, while s_2 and s_3 represent the median and the maximum values, respectively. Lastly, U is the uncertainty value (Raina & Thomas 2012; Najafi & Hessami 2017).

As the basic concepts of fuzzy logic are so simple, yet very vast, one can return to Varón-Gaviria *et al.* (2017) for the purpose of further studying.

RESULTS AND DISCUSSION

The routing process was performed on three hydrographs, which were chosen to assess the performance of the RS method.

Case Study 1

Wilson's hydrograph is chosen in this example. Wilson's is a single-peak hydrograph, which has been routed by many researchers. This hydrograph consists of 22 inflow points. In this research, for all models, the flood period is divided into three sub-regions. Each of the inflows is randomly selected and placed in a separate category. However, this RS must be such that the SSQ is minimized. Therefore, the SSQ is determined in each step and is then compared with the SSQ calculated in the previous step. The lower SSQ is reported as the outcome of the model. Table 1 provides the outflows obtained from the method, the values of k, x, and m optimized by the PSO–GA algorithm, as well as the category number, to which each point belongs. The first, second, and third categories include 6, 12, and 4 members, respectively. The values of the objective function and those of the performance indicators are presented in Table 2, in which the results from 10 different methods are compared with each other. Different methods are sorted in lines 1–10 of this table, respecting the SSQ values, i.e., the Easa

Table 1 | Comparison of routed outflows obtained from various methods for application of case study 1

		Observed data (cms)		Computed outflow (cms)	
j	Time (h)	I_j	O_j	RS	Category number
1	0	22	22	22.0	2
2	6	23	21	20.8	1
3	12	35	21	21.0	3
4	18	71	26	26.0	1
5	24	103	34	33.8	1
6	30	111	44	44.0	1
7	36	109	55	55.0	1
8	42	100	66	65.7	2
9	48	86	75	75.4	2
10	54	71	82	82.0	2
11	60	59	85	84.9	2
12	66	47	84	83.7	2
13	72	39	80	79.9	2
14	78	32	73	73.0	3
15	84	28	64	64.2	3
16	90	24	54	54.1	2
17	96	22	44	43.9	3
18	102	21	36	36.2	2
19	108	20	30	29.7	2
20	114	19	25	25.0	2
21	120	19	22	21.8	2
22	126	18	19	19.2	1
k	0.7443	0.6377	0.9352		
x	0.1767	0.2913	0.5000		
m	1.8232	1.8254	1.7805		

method has the highest SSQ value, while the lowest value of the SSQ is related to the RS method. The values of (k_i, x_i, m_i) are (0.7443, 0.6377, 0.9352), (0.1767, 0.2913, 0.5000), and (1.8232, 1.8254, 1.7805). In addition, the value of SSQ obtained from the proposed RS method is 0.6148. The lowest SSQ value ever obtained is 0.65 using Excel Solver by Bozorg-Haddad *et al.* (2020). As it turns out, the RS method has reduced the SSQ value by 5%. It is noteworthy to mention that the structure of the Muskingum model by Bozorg-Haddad *et al.* (2020) consists of eight Muskingum parameters, while in the proposed RS model, the model is made up of three Muskingum parameters. In fact, in order to make a more accurate comparison, it is necessary to compare the results of the proposed model with those from the model by Kang & Zhou (2018), which is similarly formed on three Muskingum parameters. In this model, the SSQ is 2.272, which demonstrates that the RS method has improved the value of the objective function by 73%. This implies the fact that, in both comparisons, the SSQ obtained through the RS method is the lower one. The values of five performance criteria of SAD, EQp, ETp, MARE, and VarexQ were calculated for the RS method and are also presented and compared with the performance indices of nine other methods in Table 2. As it can be inferred from the comparison, the RS method has the highest VarexQ. This index is linked with the closeness of shape and size of hydrograph. The ET_p and EQ_p represent the time and the quantity of the peak discharge, respectively. The calculated $ET_p = 0$ indicates the fact that the time of the peak discharge has not changed or shifted. In addition, the calculated $EQ_p = 0.00085$ shows that the quantity of the peak discharge has been forecasted with very little difference. The magnitude of the peak discharge equals 84.5 cms in this model, although it is 85 cms on the observational hydrograph. The MARE value of this model is 0.0034, which is lower than that of the five models listed in Table 2.

Table 2 | Performance criteria for the application of case study 1

Model	Algorithm	SSQ	SAD	EQp	ETp	MARE	VarexQ
Easa (2013)[a]	GA + GRG	24.881	20.71	0.0067	0	0.0248	99.80
Moghaddam *et al.* (2016)[b]	PSO	8.820	9.77	0.0001	0	0.015	99.93
Zhang *et al.* (2017)[c]	RAGA	5.73	8.58	0.0012	0	0.012	99.95
Farahani *et al.* (2018)[d]	Kidney	5.65	7.140	0.0004	0	0.0241	–
Farahani *et al.* (2019)[e]	Shark	5.124	8.1124	0.0002	0	0.0251	99.96
Niazkar & Afzali (2017a)[f]	MHBMO	4.043	5.967	0.0004	0	0.01	99.97
Kang & Zhou (2018)[g]	Excel Solver	2.272	5.179	NR	NR	NR	–
Akbari *et al.* (2020)[h]	PSO–GA	1.0921	3.669	0.0003	0	0.0018	99.99
Bozorg-Haddad *et al.* (2020)[k]	Excel Solver	0.65	2.66	0.0015	0	NR	NR
RS (This study)	PSO–GA	0.6148	2.8205	0.00085	0	0.0034	99.995

[a] $S_t = k(xI_t + (1-x)O_t)^{m_t}$.
[b,d,e] $S_t = k(xI_t^a + (1-x)O_t^a)^m$.
[c] $S_t = k(x(1+a)I_t + (1-x)O_t)^{m_t}$.
[g,f] $S_t = k_t(x_tI_t + (1-x_t)O_t)^{m_t}$.
[h] $S_t = k_t(x_tI_t^{a_t} + (1-x_t)O_t^{a_t})^{m_t}$.
[k] $S_t = k[x_1(c_1I_t^{\alpha_1}) + x_2(c_1I_{t+1}^{\alpha_1}) + (1-x_1-x_2)(c_2O_i^{\alpha_2})]^{\beta}$.

The uncertainty of hydrologic parameters in this case study is determined by the FAC method. Among past studies, which have been presented in Table 2, Easa (2013), Niazkar & Afzali (2017a), Kang & Zhou (2018), and the present study have employed the three-parameter nonlinear Muskingum model. The membership values (μ) were calculated based on Equation (17) for m, x, and k parameters, individually and presented in Table 3. The maximum and minimum values of each parameter were assigned 0, while the value 1 was assigned to the median. Triangular membership function graphs have been drawn for each parameter in Figure 3. The highest membership value is 1 and marks the lowest uncertainty. However, the lowest membership value, which is 0, is related to the highest uncertainty. The membership degree of the values between the minimum and the median, and the median and the maximum changes linearly from 0 to 1. This proves that the uncertainty of these values ranges from 0 to 100%. In the triangular membership function graph, the closer the supporting surface to $\propto = 0$, the greater the

Table 3 | Membership number for non-deterministic variables

Method	k	$\mu(k)$	x	$\mu(x)$	m	$\mu(m)$
Easa (2013)	0.483	0.32	0.266	0	1.906	0
	0.483	0.32	0.266	0	1.883	0.10
	0.483	0.32	0.266	0	1.884	0.1
	0.483	0.32	0.266	0	1.889	0.07
	0.483	0.32	0.266	0	1.880	0.11
Niazkar & Afzali (2017a)	1.0804	0.25	0.503	0.87	1.661	0.99
	1.686	0.38	0.382	0.95	1.627	0.96
	1.536	0.55	0.300	0.97	1.676	1
Kang & Zhou (2018)	2.021	0	0.495	0.87	1.678	1
	1.907	0.13	0.396	0.94	1.632	0.96
	1.743	0.32	0.302	1	1.646	0.97
This study	0.7443	0.59	0.6377	0.78	0.9352	0.37
	0.1767	0	0.2913	0.72	0.5	0
	1.8232	0.22	1.8254	0	1.7805	0.55
Minimum	0.1767	–	0.2660	–	0.5	–
Maximum	2.0210	–	1.8254	–	1.9060	–
Median	1.1402	–	0.3010	–	1.677	–
Uncertainty	1.4558	–	4.6627	–	0.7546	–

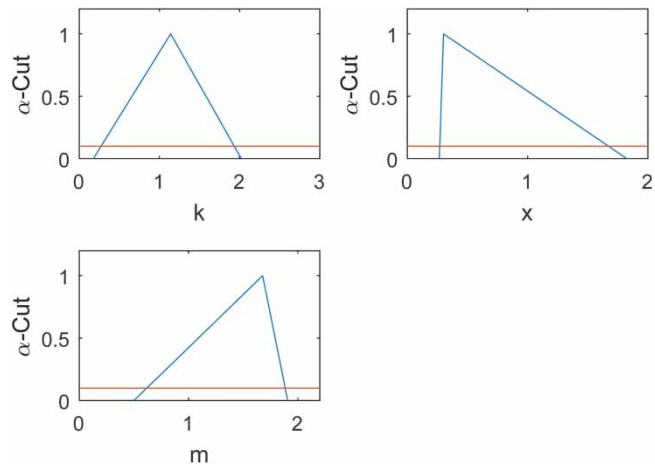

Figure 3 | Triangle membership functions for hydrologic variables.

uncertainty values, as it is inferred from width of the membership function, whereas the closer it is to the $\propto = 1$, the lower the uncertainty of the data. The maximum values of parameters k, x, and m are 2.021, 1.8254, and 1.906, respectively, while the minimum values of parameters k, x, and m are 0.1767, 0.266, and 0.5. In addition, 1.1402, 0.301, and 1.677 are the values of the median of k, x, and m, respectively. The uncertainty value in the FAC method equals the ratio of the width of the supporting surface at section $\propto = 0.1$ to the point at which the membership function value is 1. It is determined using Equation (18). The horizontal lines on Figure 3 illustrate $\propto = 0.1$. The uncertainty of the parameters x, k, and m have been determined to be 4.66, 1.46, and 0.75, respectively. Therefore, it is concluded that the uncertainty of the parameter x in flood routing is

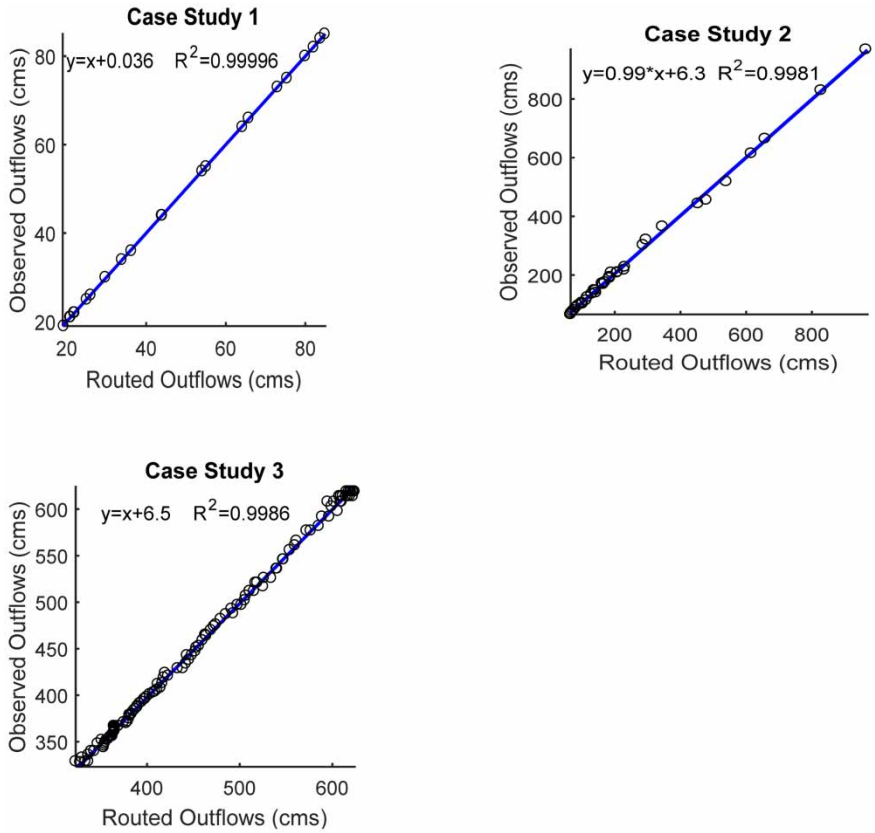

Figure 4 | Scatter plot of observed and routed outflows in three case studies.

greater than that of the parameters m and k among all methods listed in Table 3. The scatter plots of observed and routed outflows are given in Figure 4. As can be seen from the fit line equations (assume that the equation is $y = a_o x + a_1$) in the scatterplots, the a_o and a_1 coefficients are closer to the 1 and 0 with a high determination coefficient value (R^2).

Table 4 | Comparison of routed outflows obtained from various methods for the application of case study 2

		Observed data (cms)		Computed outflow (cms)	
j	Time (h)	I_j	O_j	RS	Category number
1	0	154	102	102	2
2	6	150	140	143	2
3	12	219	169	165	2
4	18	182	190	185	2
5	24	182	209	189	2
6	30	192	218	229	3
7	36	165	210	209	3
8	42	150	194	184	3
9	48	128	172	162	3
10	54	168	149	138	2
11	60	260	136	130	1
12	66	471	228	230	2
13	72	717	303	286	2
14	78	1,092	366	345	2
15	84	1,145	456	478	2
16	90	600	615	615	1
17	96	365	830	827	1
18	102	277	969	964	2
19	108	277	665	657	3
20	114	187	519	539	3
21	120	161	444	453	2
22	126	143	321	295	3
23	132	126	208	207	1
24	138	115	176	170	1
25	144	102	148	142	1
26	150	93	125	117	2
27	156	88	114	113	3
28	162	82	106	100	3
29	168	76	97	89	3
30	174	73	89	81	3
31	180	70	81	76	3
32	186	67	76	72	3
33	192	63	71	68	3
34	198	59	66	66	2
k	1.4589	1.068	1.5888		
x	0.4568	0.5350	−0.9978		
m	1.4620	1.4694	1.2681		

Case study 2

The second selected hydrograph in this paper is the one named O'Donnell (1985), which is a non-smooth hydrograph. This hydrograph belongs to a river in England. The time step in this hydrograph is 6 h and the flood period is divided into three sub-regions, and the classification criterion is the minimum value of the objective function. Table 4 shows the routed flows and the values of Muskingum parameters obtained from the RS method. In this table, the category of the inflow is given in the sixth column. In addition, each inflow can be assigned to one of three categories. The first category has six members, and each of the second and third categories has 14 members. The values of (k_i, x_i, m_i) are (1.4589, 0.4568, 1.4620), (1.068, 0.5350, 1.4694), and (1.5888, −0.9978, 1.2681), while the value of SSQ is determined to be 3733.5. In order to make a better comparison, the SSQ obtained from the other eight methods and corresponding performance indices are presented in Table 5. As can be seen, the obtained SSQ in this paper is the lowest among all these methods. It is also inferred that the RS method has reduced SSQ, whose lowest value is 9654.5, by 61.3%. Moreover, employing the RS method ends in minimum SSQ, ET_p and VarexQ values among all the models in Table 5, proving the proposed superiority of the model to them in that respect. The value of the peak discharge has been determined to be 964 cms in this method. However, the observational value of the peak discharge is 969 cms. As it is shown in Table 5. the EQ_p is 0.0048, and it is the lowest among all methods mentioned in this table. As a result, it is clear that the RS method predicts the peak discharge very accurately. In the present study, MARE, which equals 0.0391, is the least of all of the methods listed in Table 5. ET_p was determined to be 0, which proves that the model predicted the time of the peak discharge flawlessly. In Figure 4, the routed outflows are compared with the observed outflows. The coefficient of determination (R^2) values are high.

Case study 3

The inflow and outflow hydrographs, which are selected in this example, are related to the flood of the period between February 26, 2012 and March 1, 2012. The selected watershed is very similar to the Karun River watershed in terms of the morphology of the two rivers and was taken advantage of by Bazargan & Norouzi (2018) to perform the flood routing. The recorded data are extracted from the article by Bazargan & Norouzi (2018) and are given in Table 6. This hydrograph is also a single-peak hydrograph. The flood period was divided into three sub-regions, where 121 members were assigned to the categories so as to minimize the value of SSQ. Table 6 illustrates how the dataset is distributed throughout categories. The values of (k_i, x_i, m_i) are (6.5029, 6.9192, 2.7281), (0.5015, 0.4797, 0.5480), and (1.0966, 1.0896, 1.2373), and the SSQ corresponding to these Muskingum parameters is equal to 2192.8. The value of SSQ from the model by Bazargan & Norouzi (2018) is 51,301, where the objective function was set to be SAD. The values of performance indicators calculated using the RS method are SAD = 420.6, EQp = 0.0081, ETp = 4, MARE = 0.0079, and VarexQ = 99.81, which are given in Table 7. It should be noted that the maximum outflow is 619 in the observed outflow hydrograph, which occurred at nine time points. Indeed, ET_p being equal to 4 and the dislocation of the maximum by four units will not be seen as a weakness

Table 5 | Performance criteria for the application of case study 2

Model	Algorithm	SSQ	SAD	EQp	ETp	MARE	VarexQ
Easa (2013)[a]	GA + GRG	35064	NR	NR	NR	NR	NR
Easa (2014)[b]	GA + GRG	32299.2	743.32	0.078	6	0.10	98.05
Moghaddam *et al.* (2016)[c]	PSO	31099.5	695.77	0.090	6	0.09	98.12
Farahani *et al.* (2018)[d]	Kidney	16121.2	120	0.002	0	0.01	NR
Farahani *et al.* (2019)[e]	Shark	17121.2	123	0.002	2	0.01	99.11
Kang & Zhou (2018)[f]	Excel Solver	10368	NR	NR	NR	NR	NR
Akbari *et al.* (2020)[g]	PSO–GA	9654.5	392.47	0.0183	0	0.06	99.4
Bozorg-Haddad *et al.* (2020)[h]	Excel Solver	19953	621	0.071	0	NR	NR
RS (This study)	PSO–GA	3733.5	269.87	0.0048	0	0.0391	99.77

[a] $S_t = k(xI_t + (1-x)O_t)^{m_t}$.
[b,c,d,e] $S_t = k(xI_t^a + (1-x)O_t^a)^m$.
[f] $S_t = k_t(x_tI_t + (1-x_t)O_t)^{m_t}$.
[g] $S_t = k_t(x_tI_t^{a_t} + (1-x_t)O_t^{a_t})^{m_t}$.
[h] $S_t = k[x_1(c_1I_t^{\alpha_1}) + x_2(c_1I_{t+1}^{\alpha_1}) + (1-x_1-x_2)(c_2O_j^{\alpha_2})]^{\beta}$.

Table 6 | Comparison of routed outflows obtained from various methods for the application of case study 3

		Observed data (cms)		Computed outflow (cms)	
j	Time (h)	I_j	O_j	RS	Category number
1	0	376	328	328	3
2	1	381	329	333.7	3
3	2	386	329	336.7	3
4	3	391	329	323.0	1
5	4	396	333	330.1	1
6	5	401	336	336.7	1
7	6	406	340	343.1	1
8	7	411	340	339.7	2
9	8	416	348	346.9	2
10	9	429	352	351.1	2
11	10	443	356	362.7	1
12	11	456	363	364.9	1
13	12	469	367	369.3	1
14	13	482	371	374.9	1
15	14	495	379	381.1	3
16	15	508	387	389.4	1
17	16	521	396	397.9	1
18	17	529	404	408.7	1
19	18	537	412	411.6	2
20	19	545	421	422.8	3
21	20	554	429	433.1	3
22	21	562	443	443.1	3
23	22	570	451	453.1	3
24	23	578	465	462.8	3
25	24	586	474	472.2	3
26	25	594	488	493.0	2
27	26	602	497	501.9	2
28	27	610	512	510.7	2
29	28	619	521	519.0	2
30	29	627	536	539.7	1
31	30	635	546	546.7	1
32	31	643	556	553.9	1
33	32	651	566	561.2	1
34	33	649	577	572.1	1
35	34	647	582	585.3	1
36	35	644	592	596.5	1
37	36	642	598	605.7	1
38	37	636	603	599.0	2
39	38	629	608	609.0	2
40	39	623	614	616.5	2
41	40	616	614	622.1	2

(*Continued.*)

Table 6 | Continued

		Observed data (cms)		Computed outflow (cms)	
j	Time (h)	I_j	O_j	RS	Category number
42	41	610	614	609.2	3
43	42	604	619	615.1	3
44	43	598	619	619.4	3
45	44	592	619	622.1	3
46	45	586	619	623.6	3
47	46	580	619	624.0	3
48	47	574	619	623.5	3
49	48	568	619	622.2	3
50	49	562	619	620.2	3
51	50	556	619	617.6	3
52	51	550	614	614.4	3
53	52	544	614	611.3	2
54	53	537	614	607.4	3
55	54	531	614	618.8	1
56	55	525	608	610.1	1
57	56	519	608	601.8	1
58	57	510	608	594.8	1
59	58	501	592	588.8.	1
60	59	491	577	576.5	3
61	60	482	561	559.5	2
62	61	475	556	554.0	2
63	62	469	546	547.2	2
64	63	462	536	540.4	2
65	64	455	526	533.9	2
66	65	452	526	526.1	2
67	66	450	521	517.1	2
68	67	447	517	525.3	1
69	68	444	512	515.5	1
70	69	441	507	506.7	1
71	70	439	502	505.5	3
72	71	436	497	497.7	3
73	72	433	493	491.1	3
74	73	430	487	485.1	3
75	74	427	482	479.5	3
76	75	424	476	474.2	3
77	76	422	470	469.0	3
78	77	419	464	464.0	3
79	78	416	459	459.9	3
80	79	413	453	455.9	3
81	80	410	447	452.1	3
82	81	407	443	448.4	3

(*Continued.*)

Table 6 | Continued

		Observed data (cms)		Computed outflow (cms)	
j	Time (h)	I_j	O_j	RS	Category number
83	82	403	438	445.2	3
84	83	400	434	442.0	3
85	84	396	429	438.7	3
86	85	392	424	419.5	1
87	86	388	419	418.2	1
88	87	384	413	416.5	1
89	88	380	408	414.5	1
90	89	379	406	411.1	1
91	90	378	403	406.8	1
92	91	377	401	403.0	1
93	92	376	398	399.6	1
94	93	374	396	397.0	1
95	94	373	393	394.6	1
96	95	372	391	391.9	1
97	96	371	388	389.5	1
98	97	370	385	387.4	1
99	98	369	383	385.4	1
100	99	368	380	383.5	1
101	100	367	378	381.8	1
102	101	365	375	380.6	1
103	102	364	372	379.3	1
104	103	363	370	377.6	1
105	104	362	367	364.3	2
106	105	361	366	364.6	2
107	106	359	365	365.1	2
108	107	358	364	365.3	2
109	108	356	363	365.2	2
110	109	354	362	365.2	2
111	110	353	361	364.7	2
112	111	351	360	363.9	2
113	112	349	359	363.4	2
114	113	349	357	362.0	2
115	114	349	355	360.0	2
116	115	349	353	358.4	2
117	116	350	352	356.7	2
118	117	350	350	355.3	2
119	118	350	348	354.5	2
120	119	350	346	353.8	2
121	120	350	344	353.2	2
k	6.5029	0.5015	1.0966		
x	6.9192	0.4797	1.0896		
m	2.7281	0.5480	1.2373		

Table 7 | Performance criteria for the application of case study 3

Model	Algorithm	SSQ	SAD	EQp	ETp	MARE	VarexQ
Bazargan & Norouzi (2018)[a]	PSO	51301	2069.4	0.0141	1	0.04	95.7
RS (This study)[b]	PSO–GA	2192.8	420.6	0.0081	4	0.0079	99.81

[a] $S_t = k(xI_t + (1-x)O_t)$.
[b] $S_t = k_t(x_t I_t + (1-x_t)O_t)^{m_t}$.

of the model owing to the fact that the flood has a maximum value at nine time points and, above all, the peak value has not been shifted. The calculated $EQ_p = 0.0081$ shows that the quantity of the peak discharge is close to the observed peak discharge. The scatter plots of observed outflows and routed outflows are shown in Figure 4. In order to study more about the number of sub-regions, the flood period is also divided into two and four sub-regions. For $L = 2$ and $L = 4$, the values of the objective function are equal to 3565.8 and 2012.2, respectively. The results showed that increasing the number of sub-regions from 2 to 4 decreases the value of the objective function.

CONCLUSIONS

Muskingum parameters can be considered constant or variable during the flood routing process. Although the complexity of the model increases in variable-parameter flood routing, the accuracy of flood prediction increases compared to the constant-parameter routing methods. In this study, three variable parameters were considered for flood routing in the Muskingum method. The PSO–GA optimization algorithm was employed to estimate the parameters of the model. A new technique has been proposed for the classification of the sub-regions in order to increase the accuracy and improve the results of the variable-parameter Muskingum model. This technique is formed on the RS of Muskingum parameters. This way, the flood period is divided into $L = 3$ sub-regions. The sub-regions are divided in such a way that the value of the objective function is minimized. As a result, parameter selection is made randomly, and each of the inflows is placed in these categories so that the objective function is minimized. It is noteworthy that the division intervals of k, x, and m should be chosen differently to improve the results. In other words, dividing method used for sub-periods and also the number of sub-periods may differ for Muskingum parameters. For example, for k, the flood period is divided into n_k sub-period, for x, it is divided into n_x sub-period, and for m, into n_m sub-period. It is a better way to increase the accuracy of the method. The RS method was successfully tested on three models, in which the results of the RS flood routing method are compared with those of previous studies and the performance indicators are calculated. In addition, the objective function is the *SSQ* in this paper. The results show that the value of the objective function in the first, second, and the third case studies is improved by 5, 61, and 96% compared to the eight-parameter Muskingum model, four-variable-parameter Muskingum model, and three-parameter Muskingum model, respectively.

The number of previous studies indicates that increasing the accuracy of the Muskingum model has been the concern of numerous researchers. Since this method is easy to apply and also increases the accuracy of variable-parameter Muskingum models, this method can be used in all variable-parameter Muskingum models to increase their accuracy. In conclusion, the RS method is recommended in order to divide the flood period. The FAC method was used in order to investigate the uncertainty of the Muskingum parameters. This method has been used to quantify the uncertainty of the Muskingum parameters of Wilson's hydrograph. In this method, the Muskingum parameters of the three-parameter Muskingum model have been taken advantage of. The results show that the uncertainty of the parameter x is greater than that of parameters k and m.

DATA AVAILABILITY STATEMENT

All relevant data are included in the paper or its Supplementary Information.

REFERENCES

Afzali, S. H. 2016 Variable-parameter Muskingum model. *Iranian Journal of Science and Technology – Transactions of Civil Engineering* **40** (1), 59–68.

Akbari, R., Hessami-Kermani, M. R. & Shojaee, S. 2020 Flood routing: improving outflow using a new non-linear muskingum model with four variable parameters coupled with PSO-GA algorithm. *Water Resources Management* **34** (10), 3291–3316.

Barati, R. 2013 Application of excel solver for parameter estimation of the nonlinear Muskingum models. *KSCE Journal of Civil Engineering* **17** (5), 1139–1148.

Bazargan, J. & Norouzi, H. 2018 Investigation the effect of using variable values for the parameters of the linear Muskingum method using the particle swarm algorithm (PSO). *Water Resources Management* **32** (14), 4763–4777.

Bozorg-Haddad, O., Mohammad-Azari, S., Hamedi, F., Pazoki, M. & Loáiciga, H. A. 2020 Application of a new hybrid non-linear Muskingum model to flood routing. In *Proceedings of the Institution of Civil Engineers – Water Management*. Thomas Telford Ltd. Vol. 173, No. 3, pp. 109–120.

Chow, V. T., Maidment, D. R. & Mays, L. W. 1988 *Applied Hydrology*. McGraw-Hill, New York, p. 572.

Chu, H. J. & Chang, L. C. 2009 Applying particle swarm optimization to parameter estimation of the nonlinear Muskingum model. *Journal of Hydrologic Engineering* **14** (9), 1024–1027.

Easa, S. M. 2013 Improved nonlinear Muskingum model with variable exponent parameter. *Journal of Hydrologic Engineering – ASCE* **18** (22), 1790–1794.

Easa, S. M. 2014 New and improved four-parameter non-linear Muskingum model. *Proceedings of the Institution of Civil Engineers* **167** (5), 288–298.

Farahani, N. N., Farzin, S. & Karami, H. 2018 Flood routing by Kidney algorithm and Muskingum model. *Natural Hazards* 1–19. doi:10.1007/s11069-018-3482-x.

Farahani, N., Karami, H., Farzin, S., Ehteram, M., Kisi, O. & El Shafie, A. 2019 A new method for flood routing utilizing four-parameter nonlinear Muskingum and shark algorithm. *Water Resources Management* **33** (14), 4879–4893.

Garg, H. 2016 A hybrid PSO-GA algorithm for constrained optimization problems. *Applied Mathematics and Computation* **274**, 292–305.

Geem, Z. W. 2011 Parameter estimation of the nonlinear Muskingum model using parameter-setting-free harmony search. *Journal of Hydrologic Engineering* **16** (8), 684–688.

Gill, M. A. 1978 Flood routing by the Muskingum method. *Journal of Hydrology* **36** (3–4), 353–363.

Hamedi, F., Bozorg-Haddad, O., Pazoki, M., Asgari, H. R., Parsa, M. & Loaiciga, H. A. 2016 Parameter estimation of extended nonlinear Muskingum models with the weed optimization algorithm. *Journal of Irrigation and Drainage Engineering* **142** (12), 1–11.

Kang, L. & Zhou, L. 2018 Parameter estimation of variable-parameter nonlinear Muskingum model using excel solver. *IOP Conference Series: Earth and Environmental Science* **121** (5), 052047.

Karahan, H., Gurarslan, G. & Geem, Z. W. 2012 Parameter estimation of the nonlinear Muskingum flood-routing model using a hybrid harmony search algorithm. *Journal of Hydrologic Engineering* **18** (3), 352–360.

Khalifeh, S., Esmaili, K., Khodashenas, S. R. & Khalifeh, V. 2020a Estimation of nonlinear parameters of the type 5 Muskingum model using SOS algorithm. *MethodsX* **7**, 101040.

Khalifeh, S., Esmaili, K., Khodashenas, S. & Akbarifard, S. 2020b Data on optimization of the non-linear Muskingum flood routing in Kardeh River using Goa algorithm. *Data in Brief* **30**, 105398.

Kim, J. H., Geem, Z. W. & Kim, E. S. 2001 Parameter estimation of the nonlinear Muskingum model using harmony search. *JAWRA – Journal of the American Water Resources Association* **37** (5), 1131–1138.

Luo, J. & Xie, J. 2010 Parameter estimation for nonlinear Muskingum model based on immune clonal selection algorithm. *Journal of Hydrologic Engineering* **15** (10), 844–851.

Moghaddam, A., Behmanesh, J. & Farsijani, A. 2016 Parameters estimation for the new four-parameter nonlinear Muskingum model using the particle swarm optimization. *Water Resources Management* **30** (7), 2143–2160.

Mohan, S. 1997 Parameter estimation of nonlinear Muskingum models using genetic algorithm. *Journal of Hydraulic Engineering* **123** (2), 137–142.

Najafi, R. & Hessami, M. R. 2017 Uncertainty modeling of statistical downscaling to assess climate change impacts on temperature and precipitation. *Water Resources Management* **31** (6), 1843–1858.

Niazkar, M. & Afzali, S. H. 2016 Application of new hybrid optimization technique for parameter estimation of new improved version of Muskingum model. *Water Resources Management* **30** (13), 4713–4730.

Niazkar, M. & Afzali, S. H. 2017a New nonlinear variable-parameter Muskingum models. *KSCE Journal of Civil Engineering* **21** (7), 2958–2967.

Niazkar, M. & Afzali, S. H. 2017b Parameter estimation of an improved nonlinear Muskingum model using a new hybrid method. *Hydrology Research* **48** (5), 1253–1267.

Norouzi, H. & Bazargan, J. 2020 Investigation of effect of optimal time interval on the linear Muskingum method using particle swarm optimization algorithm. *Journal of Applied Research in Water and Wastewater* **7** (2), 152–156.

Norouzi, H. & Bazargan, J. 2021 Effects of uncertainty in determining the parameters of the linear Muskingum method using the particle swarm optimization (PSO) algorithm. *Journal of Water and Climate Change* **12** (5), 2055–2067.

O'Donnell, T. 1985 A direct three-parameter Muskingum procedure incorporating lateral inflow. *Hydrological Sciences Journal* **30** (4), 479–496.

Okkan, U. & Kirdemir, U. 2020 Locally tuned hybridized particle swarm optimization for the calibration of the nonlinear Muskingum flood routing model. *Journal of Water and Climate Change* **11** (S1), 343–358.

Orouji, H., Bozorg-Haddad, O., Fallah-Mehdipour, E. & Marino, M. A. 2013 Estimation of Muskingum parameter by meta-heuristic algorithms. *Proceedings of the Institution of Civil Engineers* **166** (6), 315–324.

Qiang, Z., Qiaoping, F., Xingjun, H. & Jun, L. 2020 Parameter estimation of Muskingum model based on whale optimization algorithm with elite opposition-based learning. In *IOP Conference Series: Materials Science and Engineering*. IOP Publishing. Vol. 780, No. 2, p. 022013.

Raina, R. & Thomas, M. 2012 Fuzzy vs. probabilistic techniques to address uncertainty for radial distribution load flow simulation. *Energy and Power Engineering* **4** (02), 99.

Varón-Gaviria, C. A., Barbosa-Fontecha, J. L. & Figueroa-García, J. C. 2017 Fuzzy uncertainty in random variable generation: an α-cut approach. In *International Conference on Intelligent Computing*. Springer, Cham, pp. 264–273.

Wilson, E. M. 1974 *Engineering Hydrology*. Macmillan Education LTD, Hampshire, UK.

Wu, J., Long, J. & Liu, M. 2015 Evolving RBF neural networks for rainfall prediction using hybrid particle swarm optimization and genetic algorithm. *Neurocomputing* **148**, 136–142.

Xu, G., Cui, Q., Shi, X., Ge, H., Zhan, Z. H., Lee, H. P. & Wu, C. 2019 Particle swarm optimization based on dimensional learning strategy. *Swarm and Evolutionary Computation* **45**, 33–51.

Yuan, G., Lu, J. & Wang, Z. 2021 The modified PRP conjugate gradient algorithm under a non-descent line search and its application in the Muskingum model and image restoration problems. *Soft Computing* **25** (8), 5867–5879.

Zhang, S., Kang, L., Zhou, L. & Guo, X. 2017 A new modified nonlinear Muskingum model and its parameter estimation using the adaptive genetic algorithm. *Hydrology Research* **48** (1), 17–27.

First received 29 August 2021; accepted in revised form 8 December 2021. Available online 30 December 2021